Hindawi
Mathematical Problems in Engineering
Volume 2019, Article ID 5902837, 9 pages
https://doi.org/10.1155/2019/5902837

Research Article

Face Stability Analysis of Shield Tunnel Using Slip Line Method

Weiping Liu,[1] **Shaofeng Wan**,[1] **Xinqiang Song**,[1] **Mingfu Fu**,[2] **and Lina Hu**[1]

[1]*School of Civil Engineering and Architecture, Nanchang University, Nanchang 330031, China*
[2]*School of Civil Engineering and Architecture, Nanchang Institute of Technology, Nanchang 330099, China*

Correspondence should be addressed to Weiping Liu; liuweiping@ncu.edu.cn

Received 7 July 2019; Revised 26 August 2019; Accepted 29 August 2019; Published 18 September 2019

Academic Editor: Andras Szekrenyes

The sufficient support pressure is essential to guarantee the safe construction of shield tunnel. Thus, it is necessary to analyze the stability and assess the limit support pressure of the tunnel face. The main methods for face stability analysis mostly focused on finite element method, limit equilibrium method, and numerical simulation method. In this paper, the slip line method is applied to analyze the stability of the tunnel face. The soil is supposed as ideal isotropic, homogeneous, and incompressible continuous material, which obeys the Mohr–Coulomb yield criterion. A mathematical model of the limit equilibrium boundary value problem is established. The slip line method is used to solve the slip line field and stress field of the soil behind the tunnel face. Limit support pressure and failure mechanism of the tunnel face are then obtained. In addition, comparisons between the results of this study and those of existing approach are performed, and the influence factors are also discussed. The results show that the slip line method is proven to be reliable for the evaluation of limit support pressure of the tunnel face stability.

1. Introduction

In recent years, the construction of tunnels developed rapidly in urban areas due to the continuous expansion of cities. The stability of tunneling face is an important aspect to ensure safe and controllable construction of the subway project [1]. The limit support pressure of tunnel face is one of the key factors and is one of the principles that need to be correctly evaluated for the stability of tunneling face [2]. The stability evaluation of tunnel face has been widely concerned by scholars. Kirsch [3] studied the stability of tunnel face through small-scale model tests at single gravity and the support pressure at the face in sand with different initial densities. Idinger et al. [4] investigated the face stability in a geotechnical centrifuge and analyzed the collapse at tunnel face for different overburden pressures. Dias and Bezuijen [5] proposed a path from on-site observation to realistically simulate the interaction between the tunnel boring machine and the ground.

Numerical simulation method was widely used to simulate the tunnel construction using the finite element method [6] or the finite difference method [7]. The limit support pressure and maximum surface settlement were predicted, and the stability of tunnel face was evaluated [8, 9]. Yang et al. [10] proposed a finite element upper bound solution with unstructured mesh adaption to refinement criterion, revealing the failure mechanism and evaluating stability of the tunnel face. Based on the kinematic approach of limit analysis, a continuous velocity field with a toric envelope is adopted to yield upper bounds of the tunnel face pressure for collapse [11]. Huang et al. [12] proposed a three-dimensional stability analysis of a circular tunnel face in nonhomogeneous and anisotropic undrained clay using the kinematic approach (upper bound) of limit analysis. Haghi et al. [13] developed a promoted a 3D finite element model and found that higher executed face supporting pressure could reduce the stability of the tunnel face. Chen et al. [14] proposed an improved 3D wedge-prism model which considers the height of the prism and the effect of soil arching for the analysis of tunnel face stability. Lu et al. [15] obtained the relationship between the support pressure and displacement of the shield tunnel face using the finite element method. Discrete element method was also used to analyze the stability of shield tunnel face [16–18]. Lu et al. [19] used the 3D numerical simulation method to study the effects of soil cohesion and internal friction angle on the

failure mechanism of tunnel face and the limit support pressure of the tunnel face under the specific water table line. Lee and Nam [20] studied the influence of effective stress and seepage force on the stability of tunnel face under the steady state of groundwater flow conditions. Anagnostou and Kovári [21] quantitatively discussed issues related to the impact of stand-up time, soil properties, and advance rate on the stability of tunnel face. Huang et al. [22] introduced and explored the quantitative relationship between the excavation stability of the tunnel face and the construction conditions. Dias [23] and Xu et al. [24] studied the failure mechanism of the tunnel face and the influence of tunnel depth, pore water pressure coefficient, initial cohesive force, and nonlinear coefficient on the limit support pressure. Vermeer et al. [25] and Lei et al. [26] discussed the influence of different track gradients on the limit support pressure of the tunnel face and concluded that the stability of the tunnel face can be improved by tilting the tunnel face. The limit equilibrium theory or limit analysis theory was commonly used to assess the limit support pressure of the tunnel face, and a 3D failure mechanism was proposed to study the stability of the tunnel face [27–30].

The exact numerical solution of the slip line method is fitted to the simple and analytically expressed ultimate bearing capacity formula [31]. Based on the limit equilibrium analysis method, the slip line field theory is used to analyze the ultimate bearing capacity of a pipeline [32], bearing capacity of footing [33, 34] and earth pressure on wall [35–37], and the corresponding solutions of different materials can be reasonably obtained. However, there is a lack of application of slip line method to assess the limit support pressure of tunnel face.

In this paper, the slip line method is extended to analyze the stability of the tunnel face. The mathematical model of the limit equilibrium boundary value problem is established. The slip line method is used to solve the slip line field and stress field of the soil behind the tunnel face, and the limit support pressure of tunnel face is assessed. The influence of parameters on the face stability is discussed. Moreover, comparison between the results of the present approach and existing approaches is performed.

2. Calculation Model

For tunnel construction with mud or earth pressure balance, sufficient support pressure must be specified to prevent collapse of the tunnel face. A failure mechanism model consists of a cylindrical excavation tunnel, a wedge body, and a prism body for the determination of support pressure [38], as shown in Figure 1. The wedge and the prism are the sliding body when the tunnel face loses stability. Figure 2 shows the simple calculation model for the instability of the tunnel face in an ideal situation. D is the diameter of circular tunnel. The overall thickness of cover layer is H. The crossed layer is assumed to be homogeneous. The material parameters of the soil are unit weight γ, the cohesion c, the internal friction angle φ, the external cohesion c_w, and the external friction angle δ between the tunnel face and the soil. Furthermore, supposed that the angle between the tunnel face and the x-axis is 90°, the angle between the ground and the x-axis is 0°.

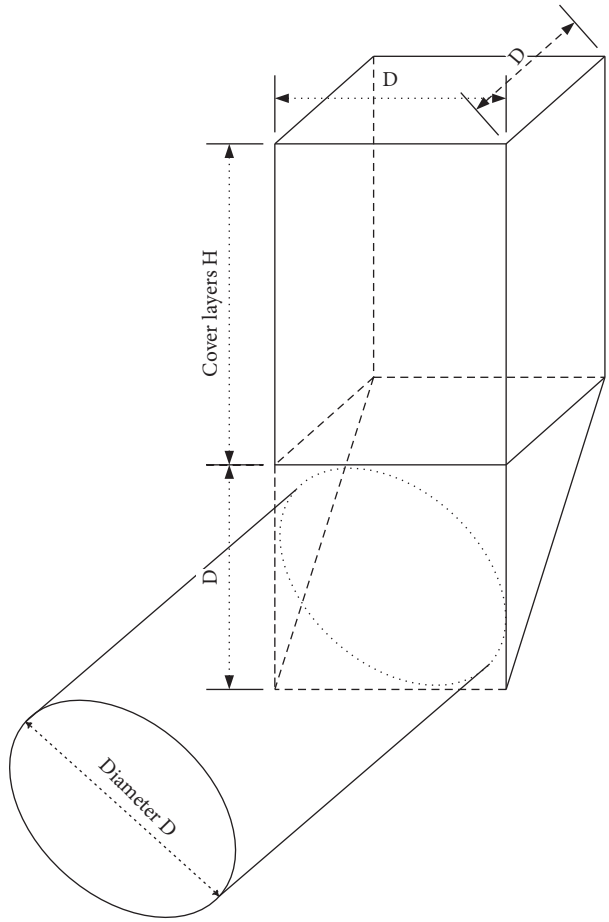

Figure 1: Failure mechanism model.

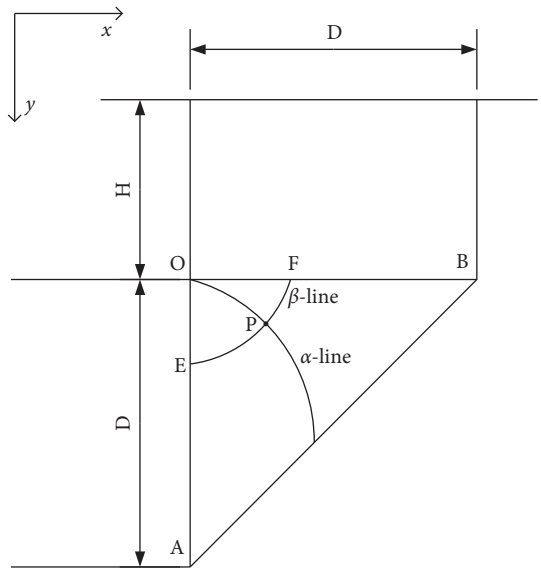

Figure 2: Calculation model.

To simplify the derivation process, the following assumptions are made: (1) considering the plane strain

problem; (2) the range of damaged tunnel face is composed of a wedge body and a prism body; (3) the top surface of the wedge body is distributed with uniform load; (4) the soil is considered to be a perfectly elastic-plastic material which obeys the Mohr–Coulomb failure criterion.

The limit Mohr circle at any point P in the plastic zone (in Figure 2) is shown in Figure 3. The α and β that get through the P point are the two slip lines and their angles with principal stress σ_1 are $\mu = (\pi/4) - (\varphi/2)$. Supposed that θ is the angle between the principal stress direction and the y-axis, then the angle between the slip lines and the y-axis are $\widetilde{\alpha} = \theta - \mu$ for α and $\widetilde{\beta} = \theta + \mu$ for β, respectively. The differential equation for slip line can be written as follows:

$$\begin{aligned} &\alpha\text{-line} : dx = \tan(\theta - \mu)dy, \\ &\beta\text{-line} : dx = \tan(\theta + \mu)dy, \end{aligned} \tag{1}$$

where θ, $\widetilde{\alpha}$, and $\widetilde{\beta}$ are the specified angle rotated from the y-axis (positive direction) and counterclockwise is regarded as the positive.

2.1. Limit Equilibrium Equation along the Slip Line. According to the limit Mohr stress circle, normal stress σ_x and σ_y and shear stress τ_{xy} can be expressed as follows:

$$\begin{cases} \sigma_x = p - R\cos 2\theta, \\ \sigma_y = p + R\cos 2\theta, \\ \tau_{xy} = R\sin 2\theta, \end{cases} \tag{2}$$

where $p = (\sigma_x + \sigma_y)/2$ is the average stress and $R = p\sin\varphi + c\cos\varphi$ is the radius of the Mohr circle. The normal stress under pressure is positive. The shear stress that makes soil rotate counterclockwise is considered to be positive. Substituting σ_x, σ_y, and τ_{xy} into the following static equilibrium equation,

$$\begin{cases} \dfrac{\partial \sigma_x}{\partial x} + \dfrac{\partial \tau_{xy}}{\partial y} = X, \\ \dfrac{\partial \tau_{xy}}{\partial x} + \dfrac{\partial \sigma_y}{\partial y} = Y, \end{cases} \tag{3}$$

where X and Y are the unit volume forces in the horizontal and vertical directions, respectively. After the simplification, the limit equilibrium equations along the α-line and the β-line are obtained:

$$\begin{cases} \cos\varphi \dfrac{dp}{ds_\alpha} - 2R\dfrac{d\theta}{ds_\alpha} = A(\theta)\cos(\theta - \mu), \\ \cos\varphi \dfrac{dp}{ds_\beta} + 2R\dfrac{d\theta}{ds_\beta} = B(\theta)\cos(\theta + \mu), \end{cases} \tag{4}$$

$$\begin{cases} A(\theta) = \dfrac{-X\cos(\theta + \mu) + Y\sin(\theta + \mu)}{\cos(\theta - \mu)}, \\ B(\theta) = \dfrac{X\cos(\theta - \mu) + Y\sin(\theta - \mu)}{\cos(\theta + \mu)}. \end{cases} \tag{5}$$

In addition, $ds_\alpha = dy/\cos(\theta - \mu)$ along the α-line and $ds_\beta = dy/\cos(\theta + \mu)$ along the β-line, and the equation (4) can be rewritten as

$$\alpha\text{-line} : \cos\varphi\, dp - 2R\, d\theta = A(\theta)dy, \tag{6}$$

$$\beta\text{-line} : \cos\varphi\, dp + 2R\, d\theta = B(\theta)dy. \tag{7}$$

2.2. Distribution of Earth Reaction Forces along the Slip Line. The earth reaction force distribution along the α-line and β-line can be calculated as follows:

$$r_\alpha = r_\beta = p - c\tan\varphi, \tag{8}$$

where the angles of the action lines of the earth pressure distribution r_α and r_β with the $+y$ direction are $\theta + \mu$ and $\theta - \mu$, respectively. It should be noted that for the entire plastic zone, the earth reaction force on the β-line OA is an external force while the rest are internal forces.

2.3. Curvature Radius of Slip Line. The curvature radius of slip line can be calculated as follows:

$$\begin{cases} R_\alpha = \dfrac{ds_\alpha}{d\theta}, \\ R_\beta = -\dfrac{ds_\beta}{d\theta}, \end{cases} \tag{9}$$

where R_α and R_β are the curvature radius of the α and β slip lines, respectively. R_α is defined as positive when the α-line concaves to $+x$ direction and R_β is positive as β-line concaves to $+y$ direction. If θ along a certain slip line remains unchanged, namely, $d\theta = 0$, then the radius of curvature is infinite.

3. Boundary Conditions

3.1. OA Stress Boundary Conditions. E is one point on the tunnel face OA, as shown in Figure 4. If the earth pressure distribution at this point is p_0, the stress components can be written as

$$\begin{cases} \sigma_n = p_0\cos^2\delta, \\ \tau_n = c_w + p_0\sin\delta\cos\delta, \end{cases} \tag{10}$$

where σ_n and τ_n are the normal stress and shear stress at point E on the boundary, respectively.

From the Mohr Circle

$$\begin{cases} \sigma_n = p_E + R_E\cos 2\left(\dfrac{\pi}{2} + \theta_E\right), \\ \tau_n = -R_E\sin 2\left(\dfrac{\pi}{2} + \theta_E\right). \end{cases} \tag{11}$$

By combining equations (10) and (11) and eliminating p_0, the stress boundary condition of the boundary OA can be written as follows:

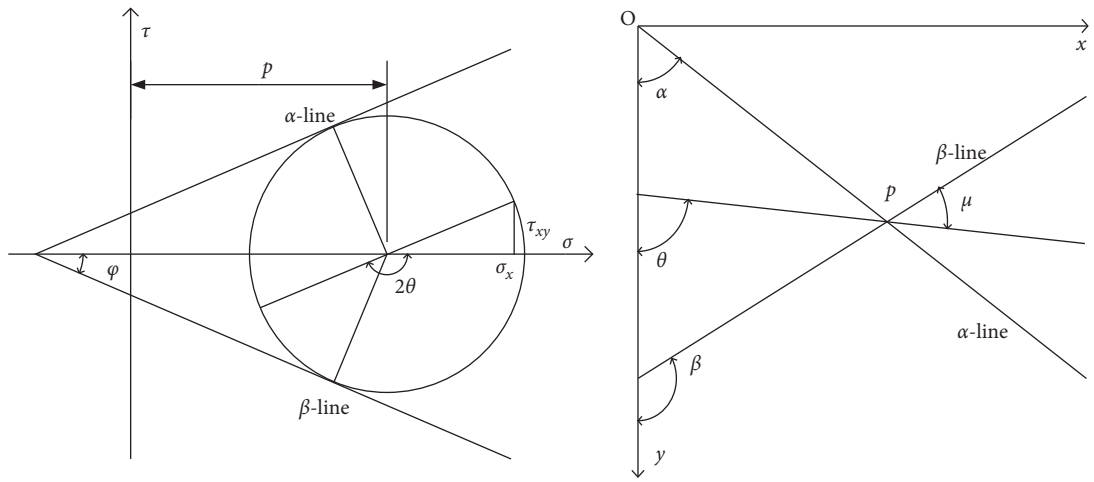

Figure 3: Limiting Mohr's stress circle at point P.

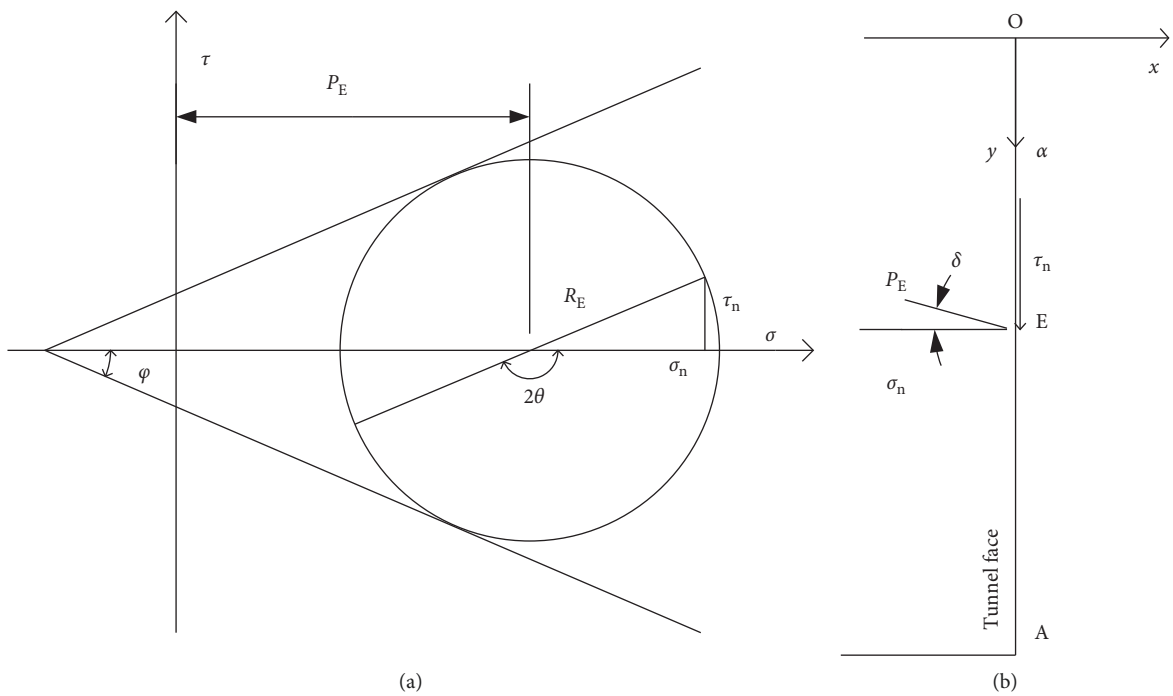

Figure 4: Limiting Mohr's stress circle at point E.

$$2\theta_E + \delta + \arcsin\left(\frac{R_w}{R_E}\right) = \pi, \tag{12}$$

where $R_E = p_E \sin\varphi + c\cos\varphi$ and $R_w = p_E \sin\delta + c_w \cos\delta$. In some special cases, the boundary condition is independent of the average stress and can be further simplified.

For example, when $c_w = 0$ and $\delta = 0$,

$$\theta_E = \frac{\pi}{2}. \tag{13}$$

When $\delta = \varphi = 0$,

$$\theta_E = \frac{\pi}{2} - \frac{1}{2}\arcsin\left(\frac{c_w}{c}\right). \tag{14}$$

When $c = c_w = 0$,

$$\theta_E = \frac{\pi}{2} - \frac{\delta}{2} - \frac{1}{2}\arcsin\left(\frac{\sin\delta}{\sin\varphi}\right). \tag{15}$$

By combining equations (10) and (11) and eliminating θ_E, a quadratic equation about p_0 can be obtained as follows:

$$p_0 = \frac{\left(p_E \cos\delta - c_w \sin\delta + R_E \cos\left(\pi + 2\theta_E + \delta\right)\right)}{\cos\delta}. \tag{16}$$

It can be seen that the earth pressure can be easily calculated by the above formula, once the average stress p_E on the boundary OA is obtained.

3.2. OB Stress Boundary Conditions. As can be seen in Figure 5, F is a point on the upper edge OB of the tunnel and q is uniform load applied to the ground. The effect of the cover layer can be considered as a distribution force [39–41].

$$\begin{cases} \sigma_n = q, \\ \tau_n = 0, \end{cases} \tag{17}$$

where

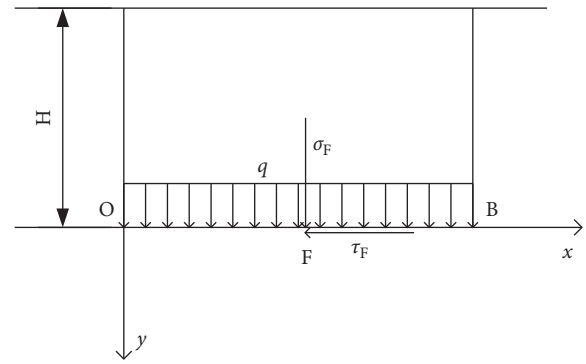

Figure 5: Limiting Mohr's stress circle at point F.

$$q = \frac{\gamma D}{4K_0 \tan\varphi}\left(1 - e^{-\left(4K_0 \tan\varphi/DH\right)}\right) - \frac{c}{K_0 \tan\varphi}\left(1 - e^{-\left(4K_0 \tan\varphi/DH\right)}\right),$$
$$K_0 = \frac{\cos^2\left((\pi/4) + (\varphi/2)\right) + \sin^2\left((\pi/4) + (\varphi/2)\right)}{\left(1 - \tan^2\left((\pi/4) + (\varphi/2)\right)\right)\sin^2\left(((\pi/4) + (\varphi/2))/3\right) + \tan^2\left(((\pi/4) + (\varphi/2))/3\right)}. \tag{18}$$

Thus,

$$\begin{aligned} \theta_F &= 0, \\ p_F &= q. \end{aligned} \tag{19}$$

3.3. O-Point Stress Boundary Conditions. When the β-line EF in Figure 2 is infinitely approaching to the O-point, the stress states of point E and F are generally different, in other words, the average stress $p_{E\longrightarrow O}$, $p_{F\longrightarrow O}$, and the direction angle $\theta_{E\longrightarrow O}$, $\theta_{F\longrightarrow O}$ are usually not the same, the point O is called the stress singularity. Setting $dy = 0$ and integrating the equation (7), the relationship between p_O and θ_O can be obtained when the β-line is infinitely close to the O-point:

$$\begin{cases} p_O = C_\beta \exp\left(-2\theta_O \tan\varphi\right) - \dfrac{c}{\tan\varphi}, \\ p_O = C_\beta - 2c\theta_O, \end{cases} \tag{20}$$

where C_β is the integral constant that needs to be determined. θ_O changes continuously between $\theta_{E\longrightarrow O}$ and $\theta_{F\longrightarrow O}$.

It can be seen that the stress singularity is the inevitable product, and the β-line degenerates from the line to the point when it is infinitely close to the point O. It is a special stress boundary with the characteristics of continuous stress, stress gradient infinity, and infinite curvature of the β-line.

4. Finite Difference Method

From the slip line equation, limit equilibrium equation, and stress boundary conditions, a complete limit equilibrium boundary value problem is formed and can generally solved by finite difference method. It is necessary to construct a finite difference mesh that consists of two groups of intersecting, imaginary slip lines before solving, as shown in Figure 6. Generally, assuming that the total number of β-lines is n, the number of nodes of the first β-line $O'O''$ is m ($m \geq 2$), then the total number of alpha lines is $2(n-2)+m$, and the total number of grid nodes is $n(n+m-1)$.

For the condition of infinitely approaching to the point O of the first β-line $O'O''$, submitting $p_{O''\longrightarrow O}$ and $\theta_{O''\longrightarrow O}$ in equation (19) into equation (20) to obtain an integral constant C_β, then the stress boundary condition of the point O is determined. In addition, combining equation (12) with (20), $p_{O'\longrightarrow O}$ and $\theta_{O'\longrightarrow O}$ can be obtained at the O' point using iterative algorithm. Considering that the $\theta_{O'\longrightarrow O}$ and $\theta_{O''\longrightarrow O}$ are not the same, this study divides the direction angle difference between $\theta_{O'\longrightarrow O}$ and $\theta_{O''\longrightarrow O}$ into $m-1$ uniform parts and assumes that the aliquot and the node corresponds to each other. Then the m nodes of the first β-line $O'O''$ are known, and the other nodes can be obtained in the same way.

5. Results and Discussion

In order to verify the results obtained from the slip line method, comparisons with existing methods [15, 27, 42–44] were conducted. A case by referring to related research analysis was carried out and calculation analysis results were as follows. Supposed parameters $H = 9\,\text{m}$, $D = 6\,\text{m}$, $\gamma = 18\,\text{kN/m}^3$, $c = 2.5\,\text{kPa}$, $\varphi = 20^\circ$, $c_w = 0\,\text{kPa}$, and $\delta = 0^\circ$, the results are shown in Figure 6.

The analysis of the limit support pressure of the tunnel face is conducted by varying the friction angle or cohesion. It can be seen from Figure 7 that the limit support pressure σ of the tunnel face is not linearly reduced with the increase of the internal friction angle of the soil. The decrease in the limit support pressure of φ from 15° and 25° is steeper than those with a range from 25° to 35°. The results obtained from slip line method were validated. The limit support pressure from this study and existing

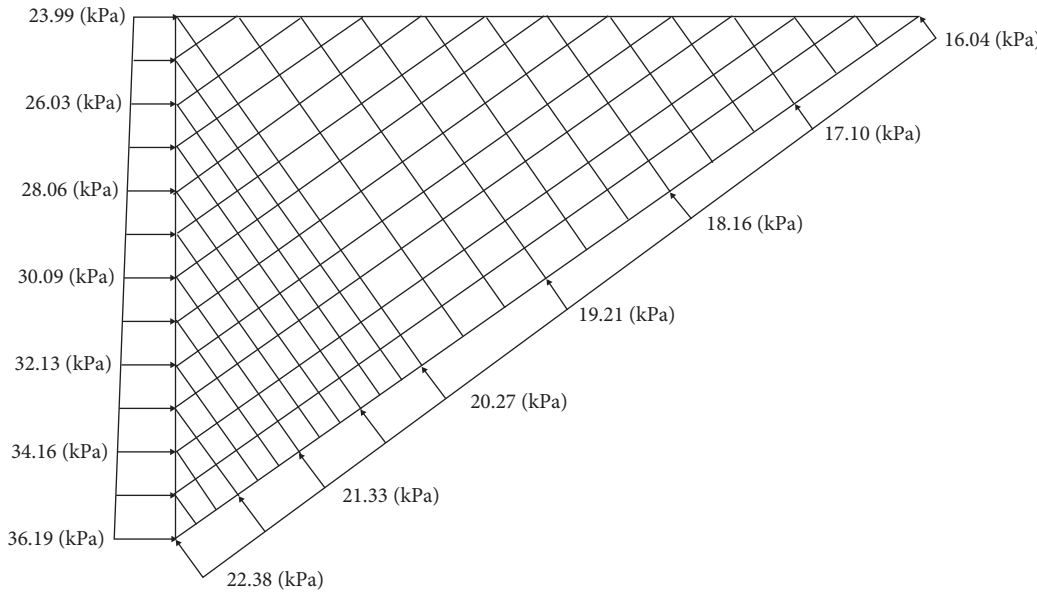

Figure 6: Results of calculation examples.

approaches are compared in Figure 7. The results of this paper are between [44] (the highest solutions) and [43] (the lowest solutions). Therefore, the slip line method provides reference for the solution of the tunnel face compared with other methods.

As shown in Figure 8 for $\varphi = 20^{\circ}$, the limit support pressure of the tunnel face decreases linearly with the increase of cohesion. Similarly, the results of this paper are between [44] (the highest solutions) and [43] (the lowest solutions). It is worth noting that the whole face of the tunnel is considered via using spatial discrete technology, which is based on the rotational face collapse mechanism proposed by Senent and Jimenez [42]. By comparing Figures 7 and 8, it is also found that the internal friction angle has a more significant impact on the limit support pressure than that of cohesion. Results show that influence rules obtained from different methods are similar. This study can consider the external friction angle and the external cohesion, and it is amenable to realistic soil behaviors.

The drawback is that, influence of the external friction angle and the external cohesion on the limit support pressure of the tunnel face and the distribution of the AB of the slip surface is not taken into account in all the results above. While Wu et al. [45] pointed out that the external friction angle is one of the important factors in the calculation of the limit support pressure of the tunnel face. Therefore, external friction angle and external cohesion are reconsidered further, and analysis about the limit support pressure and slip surface of the tunnel face is conducted in this paper. From the distribution of earth pressure at $\delta = \varphi/2$, $c_w = 0$, and the distribution of soil reaction force on the slip surface AB (in Figure 9), it can be seen that the distribution of the slip surface at this time is more in accordance with the actual situation when it comes to Figure 6.

It can be also seen in Figure 10 that the limit support pressure of the tunnel face increases with the increase of δ,

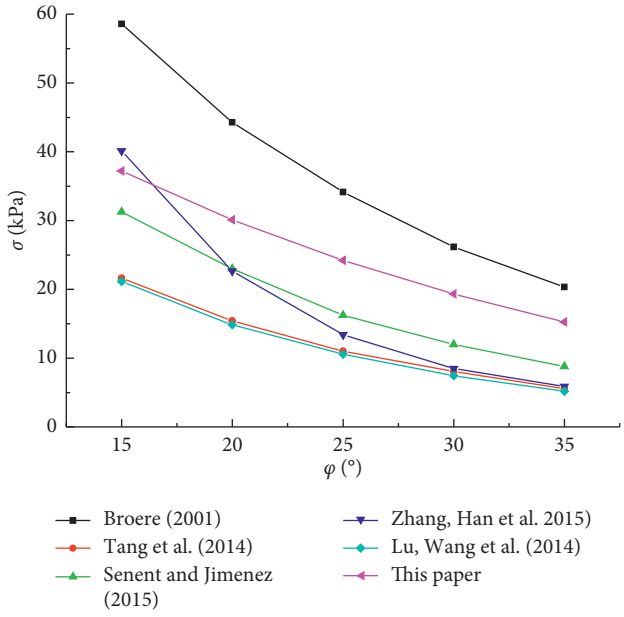

Figure 7: Influence of φ on the limit support pressures.

which is different from that of internal friction angle. Besides, the increase of the limit support pressures with δ from 10° and 20° was steeper than those with δ from 0° and 10°. Furthermore, the external friction angle has a significant impact on the limit support pressure of the tunnel face.

In Figure 11, the influence of c_w on the limit support pressure of the tunnel face is shown. It increases for increasing c_w when $\delta = 10^{\circ}$. However, as for the two factors (the external friction angle δ and the external cohesion c_w) which influence the limit support pressure of the tunnel face, the external cohesion can be negligible compared with the other one.

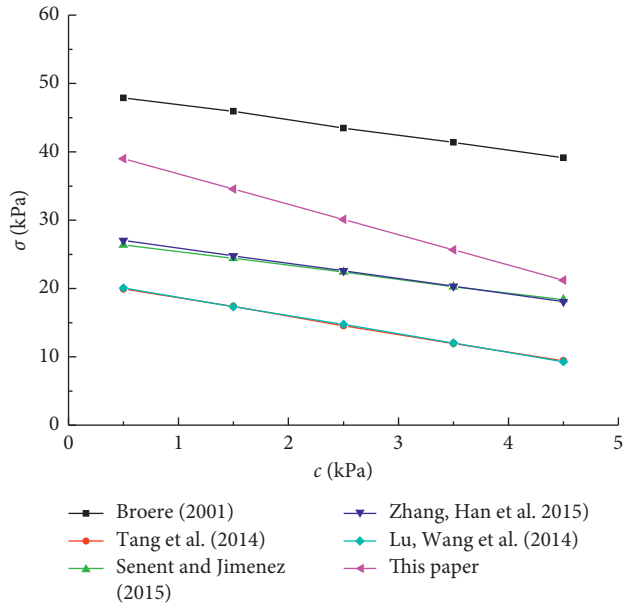

Figure 8: Influence of c on the limit support pressures.

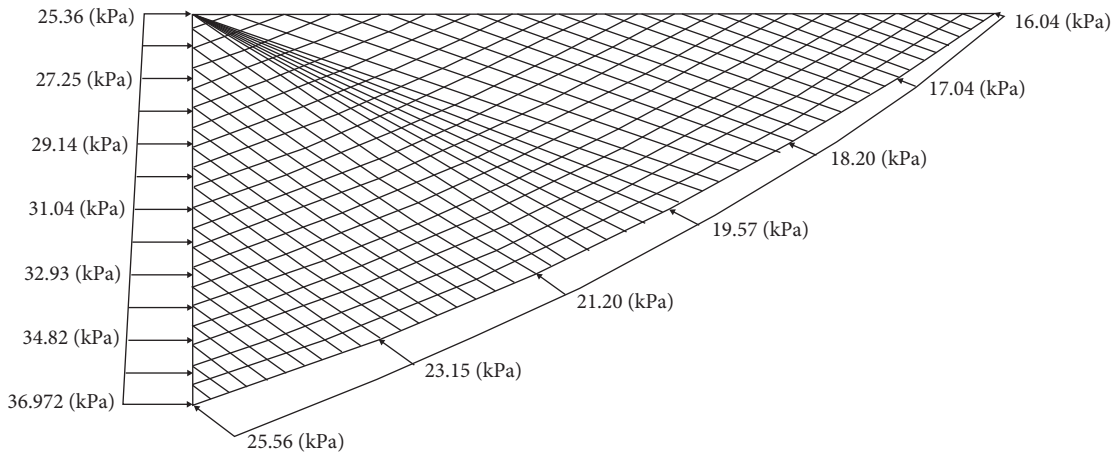

Figure 9: Results of calculation examples.

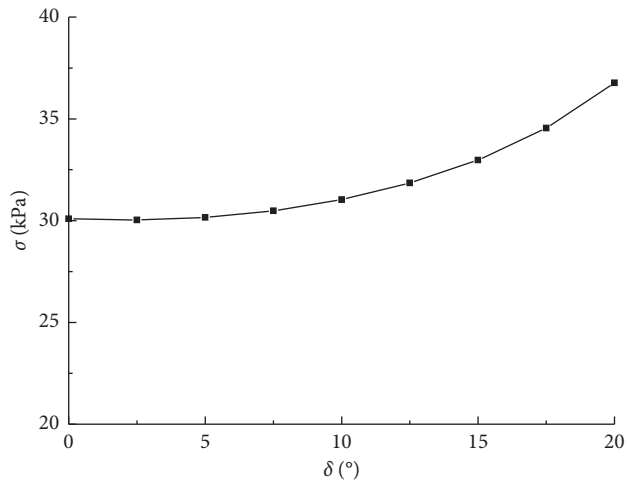

Figure 10: Influence of δ on the limit support pressures.

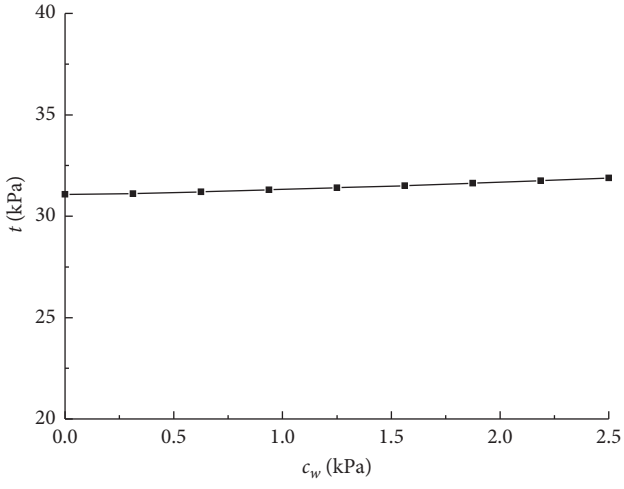

Figure 11: Influence of c_w on the limit support pressures.

6. Conclusions

Slip line method based on limit equilibrium equation is applied to analyze the limit support pressure of the tunnel face. In addition, a comparison of results between the present study and the existing methods is provided and the main conclusions are drawn as follows:

(1) The combination of the slip line method and the stress boundary condition makes the limit equilibrium problem statically solvable. There is no need to consider the stress-strain relationship of soil. The slip line and the limit equilibrium solutions are close.

(2) Under the same conditions, the limit support pressure of the tunnel face decreases linearly with the increase of the internal friction angle or cohesion, and the influence of the internal friction angle is greater than that of the cohesion.

(3) The external friction angle and the external cohesion can be considered using the slip line method. The increase of the external friction angle and the external cohesion will lead to an increase in the limit support pressure of the tunnel face. Moreover, the external friction angle has a significant influence on the limit support pressure, while the external cohesion can be negligible.

Notations

The following symbols are used in this paper:

D: Diameter of tunnel
τ_{xy}: Shear stress
H: Overall thickness of cover layer
p: Average stress
γ: Unit weight
R: Radius of the Mohr circle
c: Cohesion
X: Horizontal unit volume force
φ: Internal friction angle
Y: Vertical unit volume force
c_w: External cohesion
r_α, r_β: Earth pressure distribution
δ: External friction angle
R_α, R_β: Curvature radius
σ_1: Principal stress
p_0: Earth pressure distribution
θ: The angle between the principal stress direction and the y-axis
σ_n: Normal stress
$\widetilde{\alpha}$: The angle between the α-line and the y-axis
τ_n: Shear stress
$\widetilde{\beta}$: The angle between the β-line and the y-axis
p_E, p_F: Average stress
σ_x: Normal stress
K_0: Lateral pressure coefficient
σ_y: Vertical stress
C_β: Integral constant.

Data Availability

The data used to support the findings of this study are included within the article.

Conflicts of Interest

The authors declare that there are no conflicts of interest regarding the publication of this paper.

Acknowledgments

This research was funded by the National Natural Science Foundation of China (Grant no. 51468041) and the innovative special funds of Nanchang University (Grant no. CX2018051).

References

[1] W. Broere, "On the face support of microtunnelling TBMs," *Tunnelling and Underground Space Technology*, vol. 46, pp. 12–17, 2015.

[2] J. Mohammadi, K. Shahriar, and P. Moarefvand, "Tunnel face stability analysis in soft ground in urban tunneling by EPB shield. (case study: 7th line in Tehran Metro)," *Australian Journal of Basic & Applied Sciences*, vol. 5, no. 11, pp. 589–601, 2011.

[3] A. Kirsch, "Experimental investigation of the face stability of shallow tunnels in sand," *Acta Geotechnica*, vol. 5, no. 1, pp. 43–62, 2010.

[4] G. Idinger, P. Aklik, W. Wu, and R. I. Borja, "Centrifuge model test on the face stability of shallow tunnel," *Acta Geotechnica*, vol. 6, no. 2, pp. 105–117, 2011.

[5] T. Dias and A. Bezuijen, "TBM pressure models—observations, theory and practice," in *Proceedings of the Geotechnical Synergy in Buenos Aires 2015*, Buenos Aires, Argentina, November 2015.

[6] A. Vermeer, N. Ruse, and A. Dolatimehr, "Tunnel heading stability in drained ground," *Felsbau*, vol. 20, no. 6, pp. 8–18, 2002.

[7] H. Chakeri, Y. Ozcelik, and B. Unver, "Effects of important factors on surface settlement prediction for metro tunnel excavated by EPB," *Tunnelling and Underground Space Technology*, vol. 36, no. 2, pp. 14–23, 2013.

[8] H. R. Wang, X. L. Lu, Y. L. Liu, and M. S. Huang, "Analysis of face stability of shield tunnel under seepage condition," *Geotechnical Special Publication*, vol. 225, pp. 3209–3218, 2012.

[9] X. M. Tu, Y. Y. Yang, and G. H. Wang, "Face stability analysis of rectangular tunnels driven by a pressurized shield," *Advanced Materials Research*, vol. 378-379, no. 1, pp. 461–465, 2011.

[10] J. S. Yang, J. Zhang, and F. Yang, "Stability analysis of shallow tunnel face using two-dimensional finite element upper bound solution with mesh adaptation," *Rock & Soil Mechanics*, vol. 36, no. 1, pp. 257–264, 2015.

[11] F. Zhang, Y. F. Gao, Y. X. Wu, and N. Zhang, "Upper-bound solutions for face stability of circular tunnels in undrained clays," *Géotechnique*, vol. 68, no. 1, pp. 76–85, 2018.

[12] M. Huang, Z. Tang, W. Zhou, and J. Yuan, "Upper bound solutions for face stability of circular tunnels in non-homogeneous and anisotropic clays," *Computers and Geotechnics*, vol. 98, pp. 189–196, 2018.

[13] A. H. Haghi, M. R. Asef, A. Taheri, and M. Mohkam, "Evaluation of the heading confinement pressure effect on ground settlement for EPBTBM using full 3D numerical analysis," *International Journal of Mining and Geo-Engineering*, vol. 47, no. 1, pp. 13–32, 2013.

[14] R. P. Chen, L. J. Tang, X. S. Yin, Y. M. Chen, and X. C. Bian, "An improved 3D wedge-prism model for the face stability analysis of the shield tunnel in cohesionless soils," *Acta Geotechnica*, vol. 10, no. 5, pp. 683–692, 2015.

[15] X. Lu, H. Wang, and M. Huang, "Upper bound solution for the face stability of shield tunnel below the water table," *Mathematical Problems in Engineering*, vol. 2014, Article ID 727964, 11 pages, 2014.

[16] R. P. Chen, L. J. Tang, D. S. Ling, and Y. M. Chen, "Face stability analysis of shallow shield tunnels in dry sandy ground using the discrete element method," *Computers and Geotechnics*, vol. 38, no. 2, pp. 187–195, 2011.

[17] T. Funatsu, T. Hoshino, H. Sawae, and N. Shimizu, "Numerical analysis to better understand the mechanism of the effects of ground supports and reinforcements on the stability of tunnels using the distinct element method," *Tunnelling and Underground Space Technology*, vol. 23, no. 5, pp. 561–573, 2008.

[18] Z. X. Zhang, X. Y. Hu, and K. D. Scott, "A discrete numerical approach for modeling face stability in slurry shield tunnelling in soft soils," *Computers and Geotechnics*, vol. 38, no. 1, pp. 94–104, 2011.

[19] X. L. Lu, F. D. Li, and M. S. Huang, "Numerical simulation of the face stability of shield tunnel under tidal condition," in *Proceedings of the Geo-Shanghai*, Shanghai, China, May 2014.

[20] I.-M. Lee and S.-W. Nam, "The study of seepage forces acting on the tunnel lining and tunnel face in shallow tunnels," *Tunnelling and Underground Space Technology*, vol. 16, no. 1, pp. 31–40, 2001.

[21] G. Anagnostou and K. Kovári, "The face stability of slurry-shield-driven tunnels," *Tunnelling and Underground Space Technology*, vol. 9, no. 2, pp. 165–174, 1994.

[22] J. Huang, F. Dang, L. Zhou, K. Dang, and Y. Qin, "The quantitative analysis of the face stability on soil tunnel," *Chinese Journal of Rock Mechanics & Engineering*, vol. 35, no. S1, pp. 3127–3137, 2016.

[23] D. Dias, "Key factors in the face stability analysis of shallow tunnels," *American Journal of Applied Sciences*, vol. 10, no. 9, pp. 1025–1038, 2013.

[24] J.-S. Xu, D.-C. Du, and Z.-H. Yang, "Upper bound analysis for deep tunnel face with joined failure mechanism of translation and rotation," *Journal of Central South University*, vol. 22, no. 11, pp. 4310–4317, 2015.

[25] P. A. Vermeer, N. Ruse, and T. Marcher, "Tunnel heading stability in drained ground," *Felsbau*, vol. 20, no. 6, pp. 8–18, 2002.

[26] M. F. Lei, L. M. Peng, C. H. Shi, and D. Zhao, "Calculation and analysis of limit support force of shield tunnel excavation face under facing-slope conditions," *Chinese Journal of Geotechnical Engineering*, vol. 32, no. 3, pp. 488–492, 2010.

[27] C. Zhang, K. Han, and D. Zhang, "Face stability analysis of shallow circular tunnels in cohesive-frictional soils," *Tunnelling and Underground Space Technology*, vol. 50, pp. 345–357, 2015.

[28] Y. Li, F. Emeriault, R. Kastner, and Z. X. Zhang, "Stability analysis of large slurry shield-driven tunnel in soft clay," *Tunnelling and Underground Space Technology*, vol. 24, no. 4, pp. 472–481, 2009.

[29] K. Han, C. Zhang, W. Li, and C. Guo, "Face stability analysis of shield tunnels in homogeneous soil overlaid by multilayered cohesive-frictional soils," *Mathematical Problems in Engineering*, vol. 2016, Article ID 1378274, 9 pages, 2016.

[30] P. Perazzelli, T. Leone, and G. Anagnostou, "Tunnel face stability under seepage flow conditions," *Tunnelling and Underground Space Technology*, vol. 43, pp. 459–469, 2014.

[31] X. Daping, Z. Weiyi, and C. Huan, "Progress in slip lines method to solve the bearing capacity problem," *Chinese Journal of Geotechn Ical Engineering*, vol. 20, no. 4, pp. 28–32, 1998.

[32] F.-P. Gao, N. Wang, and B. Zhao, "Ultimate bearing capacity of a pipeline on clayey soils: slip-line field solution and FEM simulation," *Ocean Engineering*, vol. 73, no. 6, pp. 159–167, 2013.

[33] M. D. Bolton and C. K. Lau, "Vertical bearing capacity factors for circular and strip footings on Mohr-Coulomb soil," *Canadian Geotechnical Journal*, vol. 30, no. 6, pp. 1024–1033, 1993.

[34] T. Vo and A. R. Russell, "Bearing capacity of strip footings on unsaturated soils by the slip line theory," *Computers and Geotechnics*, vol. 74, pp. 122–131, 2016.

[35] F. Q. Liu and J. H. Wang, "A generalized slip line solution to the active earth pressure on circular retaining walls," *Computers and Geotechnics*, vol. 35, no. 2, pp. 155–164, 2008.

[36] F. Q. Liu, J. H. Wang, and L. L. Zhang, "Axi-symmetric active earth pressure obtained by the slip line method with a general tangential stress coefficient," *Computers and Geotechnics*, vol. 36, no. 1-2, pp. 352–358, 2009.

[37] M. X. Peng, "Slip-line solution to passive earth pressure on retaining walls," *Chinese Journal of Geotechnical Engineering*, vol. 33, no. 35, pp. 460–469, 2011.

[38] N. Horn, "Horizontaler erddruck auf senkrechte abschlussflächen von tunnelröhren," *Landeskonferenz der Ungarischen Tiefbauindustrie*, pp. 7–16, 1961.

[39] A. Kirsch and D. Kolymbas, "Theoretische Untersuchung zur Ortsbruststabilität," *Bautechnik*, vol. 82, no. 7, pp. 449–456, 2005.

[40] G. Anagnostou, "The contribution of horizontal arching to tunnel face stability," *Geotechnik*, vol. 35, no. 1, pp. 34–44, 2012.

[41] G. Anagnostou and P. Perazzelli, "The stability of a tunnel face with a free span and a non-uniform support," *Geotechnik*, vol. 36, no. 1, pp. 40–50, 2013.

[42] S. Senent and R. Jimenez, "A tunnel face failure mechanism for layered ground, considering the possibility of partial collapse," *Tunnelling and Underground Space Technology*, vol. 47, pp. 182–192, 2015.

[43] X.-W. Tang, W. Liu, B. Albers, and S. Savidis, "Upper bound analysis of tunnel face stability in layered soils," *Acta Geotechnica*, vol. 9, no. 4, pp. 661–671, 2014.

[44] W. Broere, *Tunnel Face Stability & New CPT Applications*, Delft University Press, Delft, Netherlands, 2001.

[45] J. Wu, S.-M Liao, and Z. Shi, "Workface stability of shield tunnel considering arching effect," *Journal of Tongji University (Natural Science)*, vol. 43, pp. 213–220, 2015.